Synthesis, X-Ray Characterisation and Spectroscopic Studies of Metal Complexes of *N,N'*-1,2-Xylene-α,α'-diylbis-(pyridin-2-one)*

David M. L. Goodgame, Stuart P. W. Hill, Amanda M. Smith and David J. Williams
Chemistry Department, Imperial College of Science, Technology and Medicine, London SW7 2AY, UK

The co-ordination modes adopted by *N,N'*-1,2-xylene-α,α'-diylbis(pyridin-2-one) (*o*-xbp) with Sc, Y, lanthanides, Th^{IV}, Mn^{II}, Fe^{III}, Co^{II} and Zn^{II} have been studied. Five representative complexes have been structurally characterised by single-crystal X-ray diffraction. In the monomeric ten-co-ordinate complex $[Ce(o\text{-xbp})_2(NO_3)_3]\cdot MeOH$ both *o*-xbp ligands form eleven-membered chelate rings. In the dinuclear complex $[Y_2(o\text{-xbp})_3(NO_3)_6]\cdot 3MeCN$ pairs of nine-co-ordinate Y atoms are linked by an *o*-xbp bridge, whilst the other *o*-xbp ligands form chelate rings. The dinuclear complex $[\{Zn(o\text{-xbp})Cl_2\}_2]$ forms individual 22-membered rings in which pairs of tetrahedrally co-ordinated Zn atoms are linked by *o*-xbp bridges. In the iron(III) complex $[Fe(o\text{-xbp})_2Cl_2][FeCl_4]\cdot MeOH$ the Fe atom in the cation has *cis*-octahedral co-ordination geometry with the *o*-xbp ligands forming eleven-membered chelate rings; the anion is tetrahedral. In the cobalt(II) complex $[Co(o\text{-xbp})_2(MeOH)_2]I_2\cdot 2MeOH$ the *o*-xbp ligands also chelate but the Co atom has a *trans*-octahedral geometry in which the two axial ligands are methanol molecules. A distinctive pattern of ligand conformations is observed in this series of compounds. Relevant spectroscopic results are also given.

We have recently demonstrated that extended reach bis-pyridone (**I**) or bis-lactam (**II**) ligands have appreciable potential for generating compounds with a wide variety of unusual polymeric structures.[1-3] An attractive feature of compounds of this type is the versatility of the several factors that can be exploited. A wide range of metal ions will bind to the oxygen donor atoms and therefore both the metal and the accompanying counter anion can be varied so as to modify the structure adopted. The type of bridging unit, X in **I** and **II**, can also play an important structural role, as considerable variations in the length and the geometric proclivities of the bridging unit are possible and may be utilised.

As we observed[2] that the ligand *N,N'*-1,4-xylene-α,α'-diylbis-(pyridin-2-one) (*p*-xbp, **III**) formed triple helical bridges between pairs of metal ions in the dimeric complexes $[M_2(p\text{-xbp})_3(NO_3)_6]$ (M = Pr, Nd, Sm or Er) we have explored the co-ordination behaviour of its *ortho* isomer (*o*-xbp, **IV**) towards a range of metal ions. We report here the results of this work and the structures of five representative complexes—those formed by iron(III) chloride, cobalt(II) iodide, zinc chloride, cerium(III) nitrate and yttrium nitrate.

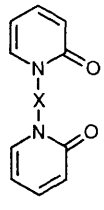

I

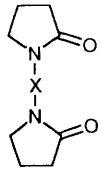

II

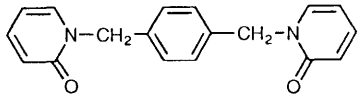

III

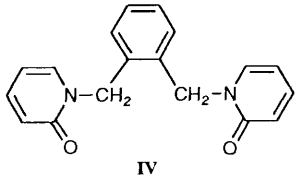

IV

Experimental

Preparation of Compounds.—N,N'-1,2-Xylene-α,α'-diylbis-(pyridin-2-one). This was obtained from the reaction of the sodium salt of pyridin-2-one with α,α'-dibromo-*o*-xylene following essentially the method of Alberti.[4] The product was extracted with hot toluene (35% yield, m.p. 167–171 °C). It crystallised with 1.5 H_2O of solvation (IR 3265 br cm^{-1}) (Found: C, 67.1; H, 5.7; N, 8.3. Calc. for $C_{18}H_{16}N_2O_2\cdot 1.5H_2O$: C, 67.7; H, 6.0; N, 8.8%). δ_H(500 MHz, $CDCl_3$) 5.26 (4 H, s), 6.23 (2 H, m), 6.65 (2H, dd), 7.07 (2 H, m), 7.28 (2H, m), 7.33 (2 H, dd) and 7.39 (2 H, m); δ_C(125 MHz, $CDCl_3$) 49.14, 106.86, 120.88, 128.48, 128.52, 134.12, 137.49, 139.93 and 162.77.

Metal complexes. The complexes obtained are listed in Table 1, together with their analytical data (Microanalytical Laboratory, Imperial College).

Scandium, yttrium, lanthanide and thorium complexes. In most cases these were prepared by mixing 0.1 mmol of the appropriate, hydrated metal salt in acetonitrile or methanol (3 cm^3) with 0.2 mmol of *o*-xbp in the same solvent (3 cm^3). The resulting solutions were allowed to concentrate gradually over concentrated sulfuric acid in a desiccator and the crystals (or powders) that formed were filtered off, washed with cold acetonitrile (or methanol, respectively) and either air-dried or dried *in vacuo* over silica gel for several hours. In the case of

* A more correct name for the ligand is *N,N'-o*-phenylenedimethylene-bis(pyridin-2-one).

Supplementary data available: see Instructions for Authors, *J. Chem. Soc., Dalton Trans.*, 1994, Issue 1, pp. xxiii–xxviii.

Table 1 Analytical data for some complexes of *N,N'*-1,2-xylene-α,α'-diylbis(pyridin-2-one) (*o*-xbp)

Complex	Solvent	Colour	Microanalysis* (%) C	H	N
$Sc(o\text{-xbp})(NO_3)_3$	MeCN	White	41.6 (41.3)	2.9 (3.1)	13.3 (13.4)
$[Y_2(o\text{-xbp})_3(NO_3)_6]\cdot 2MeCN$	MeCN	White	45.7 (46.2)	3.4 (3.0)	13.4 (13.0)
$[La(o\text{-xbp})_2(NO_3)_3]\cdot H_2O$	MeCN	White	46.4 (46.6)	3.4 (3.7)	11.1 (10.6)
$[La(o\text{-xbp})_2(NO_3)_3]$	MeOH	White	47.2 (47.5)	3.3 (3.6)	10.7 (10.8)
$[Ce(o\text{-xbp})_2(NO_3)_3]\cdot H_2O$	MeOH	White	46.7 (46.6)	3.4 (3.7)	10.7 (10.6)
$[Pr(o\text{-xbp})_2(NO_3)_3]\cdot H_2O$	MeOH	Green	46.6 (46.5)	3.3 (3.7)	10.6 (10.6)
$[Nd(o\text{-xbp})_2(NO_3)_3]\cdot H_2O$	MeOH	Mauve	46.3 (46.4)	3.4 (3.7)	10.3 (10.5)
$[Sm(o\text{-xbp})_2(NO_3)_3]\cdot H_2O$	MeOH	Cream	45.8 (46.1)	3.1 (3.7)	10.6 (10.4)
$[Sm_2(o\text{-xbp})_3(NO_3)_6]\cdot 3MeCN$	MeCN	Cream	43.2 (43.1)	3.0 (3.4)	12.7 (12.6)
$[Eu_2(o\text{-xbp})_3(NO_3)_6]\cdot 3MeCN$	MeCN	White	43.1 (43.0)	3.2 (3.4)	12.5 (12.5)
$[Gd_2(o\text{-xbp})_3(NO_3)_6]\cdot 3MeCN$	MeCN	White	42.7 (42.7)	3.1 (3.4)	12.2 (12.5)
$[Tb_2(o\text{-xbp})_3(NO_3)_6]\cdot 3MeCN$	MeCN	White	42.9 (42.6)	3.2 (3.4)	12.3 (12.4)
$[Dy_2(o\text{-xbp})_3(NO_3)_6]\cdot 3MeCN$	MeCN	White	42.6 (42.5)	3.3 (3.4)	12.5 (12.4)
$[Ho_2(o\text{-xbp})_3(NO_3)_6]\cdot 3MeCN$	MeCN	Pink	42.2 (42.3)	3.1 (3.4)	12.3 (12.3)
$[Er_2(o\text{-xbp})_3(NO_3)_6]\cdot 3MeCN$	MeCN	Pink	41.6 (42.2)	3.1 (3.4)	12.2 (12.3)
$[Tm_2(o\text{-xbp})_3(NO_3)_6]\cdot 3MeCN$	MeCN	White	42.3 (42.1)	3.2 (3.4)	12.3 (12.3)
$[Yb_2(o\text{-xbp})_3(NO_3)_6]\cdot 3MeCN$	MeCN	White	41.7 (41.9)	3.0 (3.3)	12.1 (12.2)
$[Th(o\text{-xbp})_2(NO_3)_4]\cdot MeCN$	MeCN	White	40.9 (41.3)	3.1 (3.2)	11.4 (11.4)
$La(o\text{-xbp})_2Cl_3\cdot 2H_2O\cdot 2MeOH$	MeOH	White	49.0 (49.1)	4.9 (4.8)	5.7 (6.0)
$Pr(o\text{-xbp})_2Cl_3\cdot 2H_2O\cdot MeOH$	MeOH	Green	49.7 (49.4)	4.6 (4.5)	6.4 (6.2)
$Nd(o\text{-xbp})_2Cl_3\cdot 2H_2O\cdot MeOH$	MeOH	Lilac	49.4 (49.2)	4.7 (4.5)	6.6 (6.2)
$Mn(o\text{-xbp})Cl_2\cdot MeOH$	MeCN–dmp	Cream	50.5 (50.7)	3.8 (4.5)	6.2 (6.2)
$Fe(o\text{-xbp})Cl_3\cdot 0.5MeOH$	MeCN–dmp	Orange	46.9 (47.2)	3.7 (3.9)	5.7 (6.0)
$Co(o\text{-xbp})Cl_2\cdot 0.5MeOH$	MeCN–$MeNO_2$	Dark blue	50.4 (50.7)	3.5 (4.1)	6.6 (6.4)
$Zn(o\text{-xbp})Cl_2$	MeCN–dmp	White	49.9 (50.4)	3.6 (3.8)	6.6 (6.5)
$Zn(o\text{-xbp})Br_2$	MeCN–dmp	White	41.8 (41.8)	3.1 (2.9)	5.4 (5.3)

* Calculated values are given in parentheses.

the scandium nitrate complex, equimolar amounts of the reactants were employed.

Complexes with $FeCl_3$, $ZnCl_2$ *and* $ZnBr_2$. The appropriate anhydrous metal halide (0.1 mmol) was dissolved in methanol–2,2-dimethoxypropane (dmp) (2 cm^3, 1:1) and added to a similar solution of *o*-xbp (0.1 mmol in 2 cm^3). The solution was stored in a desiccator over concentrated sulfuric acid and the crystals which formed overnight were filtered off, washed with cold dmp and air-dried. Yields: $Fe(o\text{-xbp})Cl_3\cdot 0.5MeOH$ 63% $Zn(o\text{-xbp})Cl_2$ 86%, $Zn(o\text{-xbp})Br_2$ 79%.

$Mn(o\text{-xbp})Cl_2\cdot MeOH$. This separated immediately on mixing $MnCl_2\cdot 4H_2O$ (0.1 mmol) and *o*-xbp (0.1 mmol) each dissolved in a mixture of methanol (1 cm^3) and dmp (3 cm^3). Yield 41%.

$Co(o\text{-xbp})Cl_2\cdot 0.5MeOH$. A solution of $CoCl_2\cdot 6H_2O$ (0.1 mmol) in nitromethane–methanol (6 cm^3, 2:1) was added to a solution of *o*-xbp (0.1 mmol) in nitromethane and the resulting solution allowed to concentrate as before. After a week the dark blue crystals which had formed were collected, washed with nitromethane and air-dried. Yield 77%.

$[Co(o\text{-xbp})_2(MeOH)_2]I_2\cdot 2MeOH$. Purple crystals of this complex formed on concentrating a solution of cobalt(II) iodide and *o*-xbp in 1:2 mole ratio in a mixture of methanol and dmp (2:5). These crystals were characterised by X-ray diffraction as they readily desolvated on exposure to the atmosphere.

Spectroscopy.—Spectroscopic measurements were made as previously described.[5]

Crystal Structure Determinations.—For compounds **1**–**3** and **5** data were collected on a Siemens P4 PC diffractometer using Mo-Kα radiation and the structures were solved by direct methods and refined by full-matrix least squares using anisotropic thermal parameters for the full-occupancy non-hydrogen atoms. Included solvent molecules with occupancies of less than 0.5 were refined isotropically. Hydrogen atoms for **1**–**3** were included in calculated positions, assigned isotropic thermal parameters, $U(H) = 1.2\ U_{eq}(C)$, and allowed to ride on their parent carbon atoms. For compound **5** the hydrogen atoms of the methanol molecule were located from a ΔF map and refined isotropically subject to a refined O–H distance constraint.

For compound **4** data were measured on a Siemens P3 PC diffractometer using Cu-Kα radiation and the structure was solved by the heavy-atom method. Because of the poor crystal quality, small crystal size and decomposition, the resulting number of observed data was small. Consequently, because of parameter limitations, only the iron and chlorine atoms were allowed to refine anisotropically. The C, N, and O atoms were refined isotropically. Hydrogen atoms were allowed for as for **1**–**3** above. The high final *R* factor value is a consequence of the limitations mentioned above and the large thermal anisotropy of the $FeCl_4^-$ anion.

In compound **1** two partial weight methanol molecules were located; in **2** three MeCN molecules in six partial occupancy orientations were identified; in **4** one partially disordered MeOH was observed.

A summary of the data collection and refinement parameters for all five compounds is given in Table 2. Fractional atomic co-ordinates for structures **1**–**5** are given in Tables 3, 6, 9, 11 and 13 respectively. Computations for all compounds were carried out on 486 PCs using the SHELXTL PC system.[6]

Additional material available from the Cambridge Crystallographic Data Centre comprises H-atom coordinates, thermal parameters and remaining bond lengths and angles.

Results and Discussion

Complexes of Sc^{III}, Y^{III}, Ln^{III} (Ln = *lanthanide*) *and* Th^{IV}.—Complexes of *o*-xbp with lanthanide(III) nitrates and the nitrates of Sc^{III}, Y^{III}, and Th^{IV} were readily obtained from either acetonitrile or methanol as solvent. The stoichiometry of the products depends on the metal ion. The lanthanides La–Nd gave complexes of stoichiometry $[M(o\text{-xbp})_2(NO_3)_3]$, whereas Y and Eu–Yb afforded $[M_2(o\text{-xbp})_3(NO_3)_6]$. At the transition point (Sm) use of methanol as solvent gave $[Sm(o\text{-xbp})_2(NO_3)_3]$

Table 2 X-Ray crystal data collection, solution and refinement details

Compound	**1**	**2**	**3**	**4**	**5**
Empirical formula	$C_{36}H_{32}CeN_7O_{13}$·MeOH	$C_{54}H_{48}N_{12}O_{24}Y_2$·3MeCN	$C_{36}H_{32}Cl_4N_4O_4Zn_2$	$C_{36}H_{32}Cl_6Fe_2N_4O_4$·MeOH	$C_{38}H_{40}CoI_2N_4O_6$·2MeOH
M	942.8	1550.0	857.2	941.1	1025.6
Colour, habit	Clear plates	Colourless, prismatic plates	Clear, needles	Orange, platy needles	Purple plates
Crystal system	Triclinic	Monoclinic	Monoclinic	Monoclinic	Monoclinic
Crystal size/mm	0.12 × 0.33 × 0.36	0.118 × 0.334 × 0.367	0.30 × 0.33 × 0.67	0.043 × 0.26 × 0.78	0.08 × 0.47 × 0.67
Space group	$P\bar{1}$	$C2/c$	$P2_1/c$	$P2_1/c$	$C2/c$
a/Å	9.806(8)	24.992(14)	9.203(4)	16.140(15)	21.255(7)
b/Å	11.170(9)	16.299(7)	19.470(6)	10.577(10)	9.215(4)
c/Å	19.890(16)	17.104(9)	10.268(6)	25.91(4)	23.605(8)
α/°	102.57(2)	—	—	—	—
β/°	96.16(2)	100.24(2)	102.98(2)	104.13(2)	113.03(2)
γ/°	105.16(2)	—	—	—	—
U/Å^3	2021(3)	6857(9)	1792.8(14)	4290(8)	4255(3)
Z	2	4[a]	2[b]	4	4[a]
D_c/g cm^{-3}	1.549	1.502	1.588	1.457	1.601
μ/mm^{-1}	1.20	1.77	1.68	9.23	1.91
$F(000)$	954	3168	872	1920	2052
2θ Range/°	4–50	4–45	3–50	0–100	0–48
Independent reflections (R_{int})	7131 (0.00)	4486 (0.026)	3161 (0.020)	4406 (0.045)	3347 (0.021)
Observed reflections [$F_o > 4\sigma(F_o)$]	5142	2458	2555	1606	2346
Min., max. transmission	—	0.593, 0.817	—	0.221, 0.832	0.565, 0.889
g in weighting scheme[c]	0.0006	0.0005	0.0006	0.0010	0.0006
No. of parameters refined	541	452	227	257	257
Final R (R')	0.0530 (0.0501)	0.0523 (0.0446)	0.0315 (0.0340)	0.136 (0.127)	0.0434 (0.0436)
Largest and mean Δ/σ	0.935, 0.018	0.038, 0.002	0.000, 0.000	0.346, 0.023	0.021, 0.001
Data/parameter ratio	9.5:1	5.4:1	11.3:1	6.2:1	9.1:1
Largest difference peak, hole/e Å^{-3}	0.86, −1.11	0.33, −0.41	0.37, −0.36	1.41, −1.21	0.82, −0.64

Details in common: room temperature; numerical absorption correction (face-indexed crystals).
[a] The complex has crystallographic C_2 symmetry. [b] The complex has crystallographic C_i symmetry. [c] $w^{-1} = \sigma^2F + gF^2$.

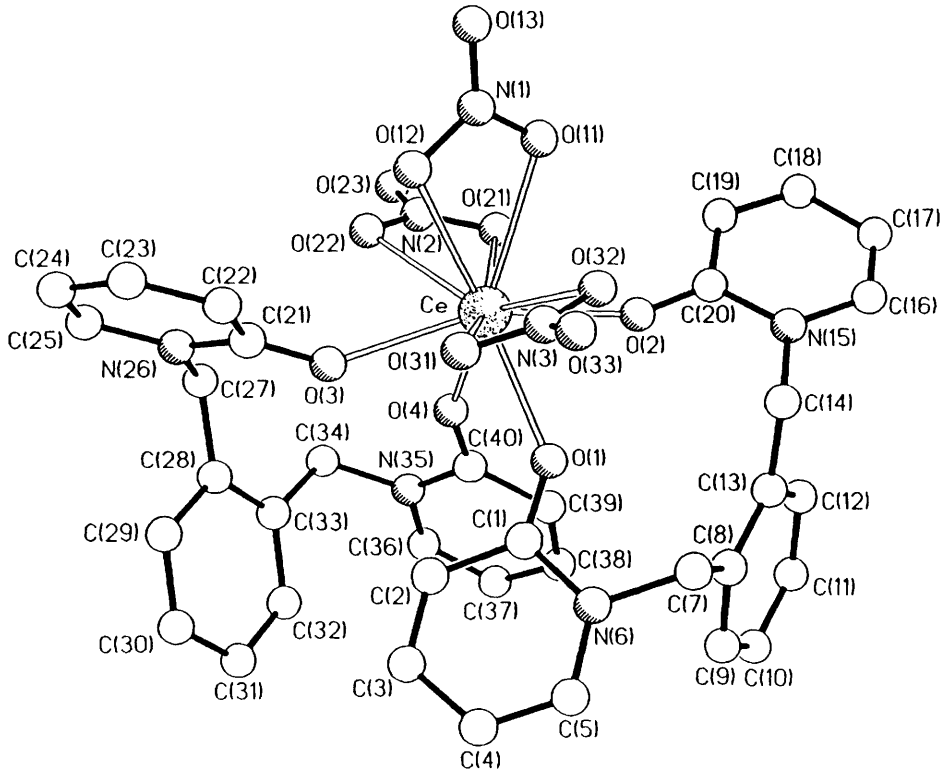

Fig. 1 The molecular structure of complex **1**

whereas $[Sm_2(o\text{-xbp})_3(NO_3)_6]$ was obtained from acetonitrile.

Solvation seems to be a prevalent feature in this series of complexes and the choice of solvent influences the yields and crystallinity of the products as well as the nature of occluded solvent or water molecules. Use of acetonitrile for Y and Sm–Yb gave high yields (87–100%) of the complexes $[M_2(o\text{-xbp})_3(NO_3)_6]$, as acetonitrile solvates, in good crystalline form, but there was slow loss of the occluded acetonitrile after the crystals were isolated from solution (*e.g.* analytical results for the yttrium complex were consistent with partial loss of the acetonitrile molecules found by the X-ray study on the crystals, see below). For La–Nd the products from acetonitrile were obtained in comparatively poorer yields (34–60%) and only as fine powders, which on removal from the mother-liquor and exposure to air rapidly lost any acetonitrile of solvation and formed hydrates $[M(o\text{-xbp})_2(NO_3)_3]\cdot nH_2O$ (n = 1 or 1.5). Use of methanol as solvent, however, gave good crystals of the complexes of La–Nd and in better yields (*ca.* 70%). As shown from the X-ray structural analysis of the cerium complex (see below) the crystals contain methanol of solvation when first isolated from solution, but they desolvate and form monohydrates on storage in air.

X-Ray powder photographs showed that the compounds $[M(o\text{-xbp})_2(NO_3)_3]$(M = La–Nd) obtained from methanol form an isostructural series, and this is also the case for the series $[M_2(o\text{-xbp})_3(NO_3)_6]$(M = Y and Sm–Yb) obtained from acetonitrile. Representative members from these two series, $[Ce(o\text{-xbp})_2(NO_3)_3]\cdot MeOH$ **1** and $[Y_2(o\text{-xbp})_3(NO_3)_6]\cdot 3MeCN$ **2**, were fully characterised by single-crystal X-ray diffraction studies.

Structure of $[Ce(o\text{-xbp})_2(NO_3)_3]\cdot MeOH$ **1**.—The X-ray analysis of **1** shows it to have a discrete monomeric molecular structure in which each Ce atom is ten-co-ordinate, being bound to six oxygen atoms from three bidentate nitrate groups and four oxygen atoms from two chelating *o*-xbp ligands (Fig. 1).

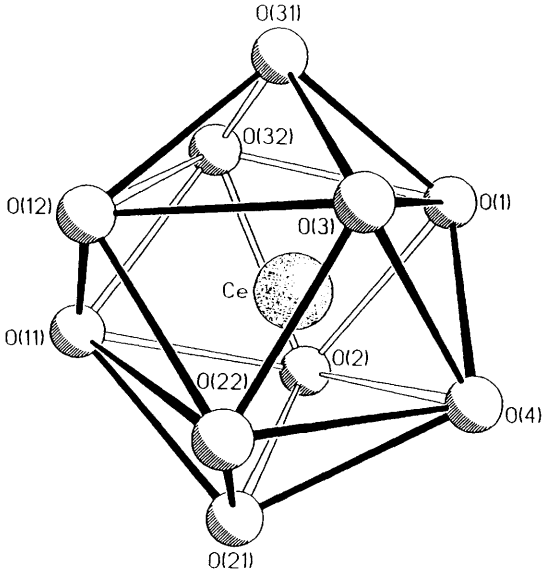

Fig. 2 The distorted bicapped square-antiprismatic co-ordination about the cerium atom in **1**

The Ce–O(pyridone) distances are in the range 2.40–2.48 Å and the Ce–O(nitrate) distances are 2.61–2.73 Å (Table 4).

The co-ordination geometry around the cerium atom may be considered as distorted bicapped square antiprismatic (Fig. 2) with the nitrate oxygen atoms O(21) and O(31) as the capping atoms. This geometry is similar to that observed previously for the 2-pyrrolidonate complex $[\{Hg_2Th(C_4H_6NO)_4(NO_3)_4\}_n]$[7] and the 2-pyridone complex $[Th(C_5H_5NO)_6(NO_3)_2][NO_3]_2$.[8] Alternatively, if one considers the nitrate groups as each occupying a *single* co-ordination position a pentagonal-bipyramidal geometry results, in which O(2) and O(3) occupy

Table 3 Atomic coordinates (× 10^4) for compound **1**

Atom	*x*	*y*	*z*	Atom	*x*	*y*	*z*
Ce	1 267(1)	8 819(1)	2 505(1)	C(27)	3 366(8)	8 047(7)	4 467(4)
O(1)	85(5)	6 622(5)	1 754(3)	C(28)	2 599(8)	6 611(7)	4 265(4)
O(2)	−1 003(5)	8 852(5)	1 937(3)	C(29)	3 370(9)	5 734(8)	4 101(5)
O(3)	2 982(5)	8 050(4)	3 116(3)	C(30)	2 718(9)	4 431(8)	3 902(5)
O(4)	−99(5)	7 608(5)	3 229(3)	C(31)	1 284(9)	3 946(8)	3 860(5)
C(1)	184(8)	5 507(7)	1 652(4)	C(32)	522(9)	4 811(8)	4 042(4)
C(2)	999(9)	5 054(8)	2 107(4)	C(33)	1 159(8)	6 126(7)	4 242(3)
C(3)	1 070(10)	3 851(9)	1 953(5)	C(34)	224(8)	6 997(8)	4 451(4)
C(4)	334(11)	2 992(9)	1 307(5)	N(35)	−1 144(6)	6 542(6)	3 977(3)
C(5)	−467(10)	3 377(8)	873(5)	C(36)	−2 279(9)	5 752(9)	4 147(5)
N(6)	−545(6)	4 609(6)	1 030(3)	C(37)	−3 470(10)	5 157(9)	3 694(6)
C(7)	−1 448(8)	5 040(8)	539(4)	C(38)	−3 569(10)	5 368(10)	3 027(6)
C(8)	−2 814(8)	5 132(7)	784(4)	C(39)	−2 442(9)	6 193(9)	2 845(5)
C(9)	−3 693(10)	4 053(9)	925(4)	C(40)	−1 180(8)	6 825(7)	3 326(4)
C(10)	−4 978(10)	4 042(10)	1 121(5)	N(1)	3 170(9)	11 415(7)	2 410(4)
C(11)	−5 416(10)	5 121(11)	1 181(5)	O(11)	1 848(7)	11 147(6)	2 311(4)
C(12)	−4 571(9)	6 215(9)	1 040(4)	O(12)	3 670(6)	10 565(6)	2 573(4)
C(13)	−3 255(8)	6 231(8)	838(4)	O(13)	3 934(8)	12 433(6)	2 363(5)
C(14)	−2 379(9)	7 433(7)	663(4)	N(2)	1 136(8)	10 655(6)	3 912(4)
N(15)	−2 652(7)	8 626(6)	1 011(3)	O(21)	192(6)	10 391(5)	3 391(3)
C(16)	−3 677(11)	9 076(11)	708(5)	O(22)	2 200(7)	10 259(6)	3 816(3)
C(17)	−3 946(12)	10 141(11)	1 004(6)	O(23)	1 025(9)	11 269(8)	4 480(3)
C(18)	−3 161(11)	10 880(9)	1 665(5)	N(3)	2 488(8)	8 206(7)	1 114(4)
C(19)	−2 136(9)	10 473(8)	1 974(4)	O(31)	2 955(6)	7 932(7)	1 633(3)
C(20)	−1 869(8)	9 312(7)	1 667(4)	O(32)	1 546(7)	8 801(7)	1 191(3)
C(21)	4 262(7)	8 343(6)	3 402(4)	O(33)	2 886(8)	7 960(8)	543(3)
C(22)	5 445(8)	8 645(8)	3 056(4)	O(50)	5 522(15)	12 000(11)	3 934(5)
C(23)	6 787(9)	8 937(8)	3 400(5)	C(50)	6 834(20)	12 180(13)	3 723(8)
C(24)	7 048(9)	8 964(8)	4 106(5)	O(60)	1 595(33)	10 635(29)	380(16)
C(25)	5 948(8)	8 687(7)	4 444(4)	C(60)	472(24)	10 069(28)	28(15)
N(26)	4 564(6)	8 372(5)	4 100(3)				

Table 4 Selected bond lengths (Å) and angles (°) with estimated standard deviations (e.s.d.s) in parentheses for complex **1**

Ce–O(1)	2.478(5)	Ce–O(2)	2.398(6)
Ce–O(3)	2.411(6)	Ce–O(4)	2.452(6)
Ce–O(11)	2.636(7)	Ce–O(12)	2.606(6)
Ce–O(21)	2.705(7)	Ce–O(22)	2.668(6)
Ce–O(31)	2.731(7)	Ce–O(32)	2.653(7)
O(1)–Ce–O(2)	73.7(2)	O(1)–Ce–O(3)	90.5(2)
O(2)–Ce–O(3)	158.8(2)	O(1)–Ce–O(4)	73.3(2)
O(2)–Ce–O(4)	86.4(2)	O(3)–Ce–O(4)	75.4(2)
O(1)–Ce–O(11)	135.1(2)	O(2)–Ce–O(11)	77.3(2)
O(3)–Ce–O(11)	123.7(2)	O(4)–Ce–O(11)	137.9(2)
O(1)–Ce–O(12)	134.3(2)	O(2)–Ce–O(12)	123.1(2)
O(3)–Ce–O(12)	78.0(2)	O(4)–Ce–O(12)	141.5(2)
O(11)–Ce–O(12)	47.4(2)	O(1)–Ce–O(21)	129.9(2)
O(2)–Ce–O(21)	70.5(2)	O(3)–Ce–O(21)	112.2(2)
O(4)–Ce–O(21)	70.6(2)	O(11)–Ce–O(21)	67.4(2)
O(12)–Ce–O(21)	94.8(2)	O(1)–Ce–O(22)	145.4(2)
O(2)–Ce–O(22)	116.8(2)	O(3)–Ce–O(22)	69.1(2)
O(4)–Ce–O(22)	74.6(2)	O(11)–Ce–O(22)	78.7(2)
O(12)–Ce–O(22)	70.1(2)	O(21)–Ce–O(22)	46.3(2)
O(1)–Ce–O(31)	66.8(2)	O(2)–Ce–O(31)	115.3(2)
O(3)–Ce–O(31)	68.9(2)	O(4)–Ce–O(31)	125.0(2)
O(11)–Ce–O(31)	96.9(2)	O(12)–Ce–O(31)	67.9(2)
O(21)–Ce–O(31)	162.4(2)	O(22)–Ce–O(31)	125.1(2)
O(1)–Ce–O(32)	71.1(2)	O(2)–Ce–O(32)	74.0(2)
O(3)–Ce–O(32)	114.7(2)	O(4)–Ce–O(32)	143.0(2)
O(11)–Ce–O(32)	68.4(2)	O(12)–Ce–O(32)	74.1(2)
O(21)–Ce–O(32)	127.8(2)	O(22)–Ce–O(32)	142.3(2)
O(31)–Ce–O(32)	46.0(2)	Ce–O(1)–C(1)	141.1(5)
Ce–O(2)–C(20)	156.8(5)	Ce–O(3)–C(21)	143.4(5)
Ce–O(4)–C(40)	152.8(5)	Ce–O(11)–N(1)	98.3(6)
Ce–O(12)–N(1)	99.0(5)	Ce–O(21)–N(2)	97.9(5)
Ce–O(22)–N(2)	99.4(4)	Ce–O(31)–N(3)	98.1(6)
Ce–O(32)–N(3)	100.3(5)		

the axial positions. (The equatorial groups subtend angles of between 66 and 78°.)

A noticeable feature of the ligand dispositions is the way in which the two *o*-xbp units are grouped in one co-ordination hemisphere and the nitrates in the other. The complex has approximate, non-crystallographic, molecular C_2 symmetry about an axis passing through N(1), the cerium atom, and bisecting the O(1)–Ce–O(4) and O(2)–Ce–O(3) angles. The conformations of the *o*-xbp ligands are very similar, both having approximate C_s symmetry; the principal torsion angles are given in Table 5.

Inter-ligand stabilisation is provided by pyridone–xylyl ring edge-to-face interactions. These occur between the pyridone ring [C(1)–N(6)] and the xylyl ring [C(28)–C(33)] and between the pyridone [N(35)–C(40)] and the aryl [C(8)–C(13)]. The centroid–centroid ring separations are 5.00 and 4.93 Å respectively, and the centroid–centroid vectors subtend angles of 74 and 80° to the respective xylene ring planes.

There are no important intermolecular packing interactions. The partial occupancy, included methanol molecules form weak O–H···O hydrogen bonds to the nitrate groups. As mentioned previously, these solvent molecules are readily lost from the crystals on storage in air, and the compound forms a hydrate.

Structure of $[Y_2(o\text{-xbp})_3(NO_3)_6]\cdot 3MeCN$ **2**.—The X-ray study of **2** shows it to consist of discrete $[Y_2(o\text{-xbp})_3(NO_3)_6]$ dinuclear units in which the pairs of yttrium atoms are bridged by one *o*-xbp ligand (Fig. 3). Each Y atom is nine-co-ordinate and has bonded to it six oxygen atoms from three bidentate nitrates and three pyridone oxygen atoms, one of which is provided by the *o*-xbp bridge, the other two coming from a chelating *o*-xbp ligand (Fig. 4). The co-ordination geometry about each Y atom can be considered as very distorted monocapped square antiprismatic with the nitrate oxygen O(21) acting as the capping atom (Fig. 5).

The Y–O(pyridone) distances are in the range 2.24–2.26 Å, while the Y–O(nitrate) distances are 2.41–2.51 Å (Table 7). These distances are consistently shorter than those in

Table 5 Comparative torsional relationships between the aromatic rings in the *o*-xbp ligands in **1**–**5*** [Torsion angles (°) have been normalised to correspond with a single enantiomeric ligand conformation]

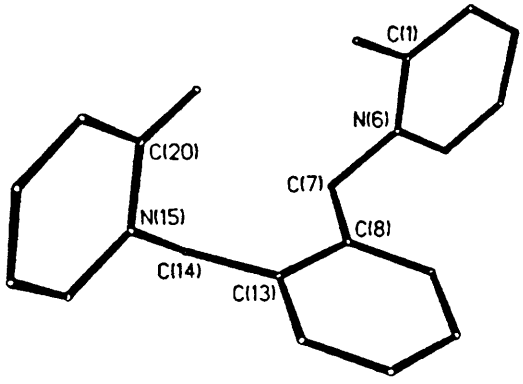

	1		2		3	4		5
C(1)–N(6)–C(7)–C(8)	−75	−74	−80	−96	−80	−74	−73	−78
N(6)–C(7)–C(8)–C(13)	129	147	150	181	127	124	158	117
C(8)–C(13)–C(14)–N(15)	−156	−140	−134	—	−135	−155	−120	−164
C(13)–C(14)–N(15)–C(20)	88	79	79	—	58	77	77	80

* The second column for compounds **1** and **4** refers to the non-symmetry related ligand. For compound **2** this column corresponds to the geometry of the unique portion of the C_2 symmetric bridge ligand.

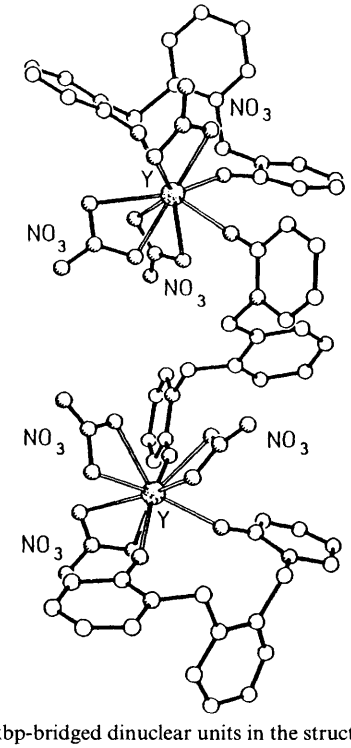

Fig. 3 The *o*-xbp-bridged dinuclear units in the structure of **2**

1 reflecting both the smaller metal ion size and the lower co-ordination number.

The geometry of the chelating *o*-xbp ligand in **2** is very similar to that observed in **1**, again approximating to C_s symmetry. However the bridging ligand in **2**, whilst still retaining an essentially orthogonal relationship between the *o*-xylene and pyridone rings, has crystallographic C_2 symmetry (torsion angles are listed in Table 5).

There are no significant inter- or intra-molecular interactions.

The difference in structural type between the two groups of compounds, $[M(o\text{-xbp})_2(NO_3)_3]$ and $[M_2(o\text{-xbp})_3NO_3)_6]$ may be attributed to a balance between the proclivity of these metal ions to achieve high co-ordination numbers (and to utilise the chelating ability of the nitrate ions to achieve this) and the steric effects of a reduction in the size of the metal ion. Cerium(III) and the other lanthanide ions in the first part of the series (La–Sm) are able to accommodate two chelating *o*-xbp ligands as well as three bidentate nitrates, and, from the stoichiometry, chelation also appears to occur with Th^{IV}. The smaller ionic size of Y, and also of the later members of the lanthanides (Eu–Yb), results in a reduction from four to three pyridone units being bonded to the metal centre. The fact that this bonding takes the form of one chelating and one bridging *o*-xbp ligand, instead of all ligands bridging and forming a more extended polymeric array, suggests that the *o*-xylenediyl link favours chelation despite the large size (eleven-membered) of the resulting chelate rings. This, in turn, may be associated with the predeliction for the *o*-xbp ligand to retain an orthogonal relationship of the pyridone rings with respect to the *o*-xylene ring (see above). Further reduction in metal ion size to that of Sc^{III} results in the formation of a 1:1 complex $[Sc(o\text{-xbp})(NO_3)_3]$, most probably containing chelating *o*-xbp.

Reactions between *o*-xbp and hydrated $LnCl_3$ (Ln = La, Pr or Nd) in methanol gave the compounds $Ln(o\text{-xbp})_2Cl_3\cdot 2H_2O\cdot n MeOH$ (La, $n = 2$; Pr, Nd, $n = 1$), but these have not been structurally characterised by X-ray methods.

Four of the solid lanthanide nitrate complexes $[M_2(o\text{-xbp})_3(NO_3)_6]$ (M = Sm, Eu, Tb, Dy) luminesce under near-UV excitation and their phosphorescent emission properties are summarised in Table 8. (The luminescence of the Sm complex was considerably weaker than for the other three complexes.)

Transition-metal Halide Complexes.—Reaction of the chlorides of Mn^{II}, Fe^{III}, Co^{II} or Zn^{II}, and also zinc(II) bromide, with *o*-xbp in a mixture of methanol and 2,2-dimethoxypropane or, for cobalt(II) chloride, in methanol–nitromethane, gave complexes with a 1:1 *o*-xbp:M ratio (Table 1).

The electronic spectrum of the dark blue cobalt complex is typical of a slightly distorted tetrahedral (C_{2v}) metal co-ordination geometry,[9] with strong bands in the near infrared [5400, 6170, 7610 cm^{-1}, transitions to components of $^4T_1(F)$] and visible [15 700 cm^{-1} (multicomponent), transitions to components of $^4T_1(P)$] regions. Additional evidence for essentially tetrahedral $CoCl_2O_2$ co-ordination comes from

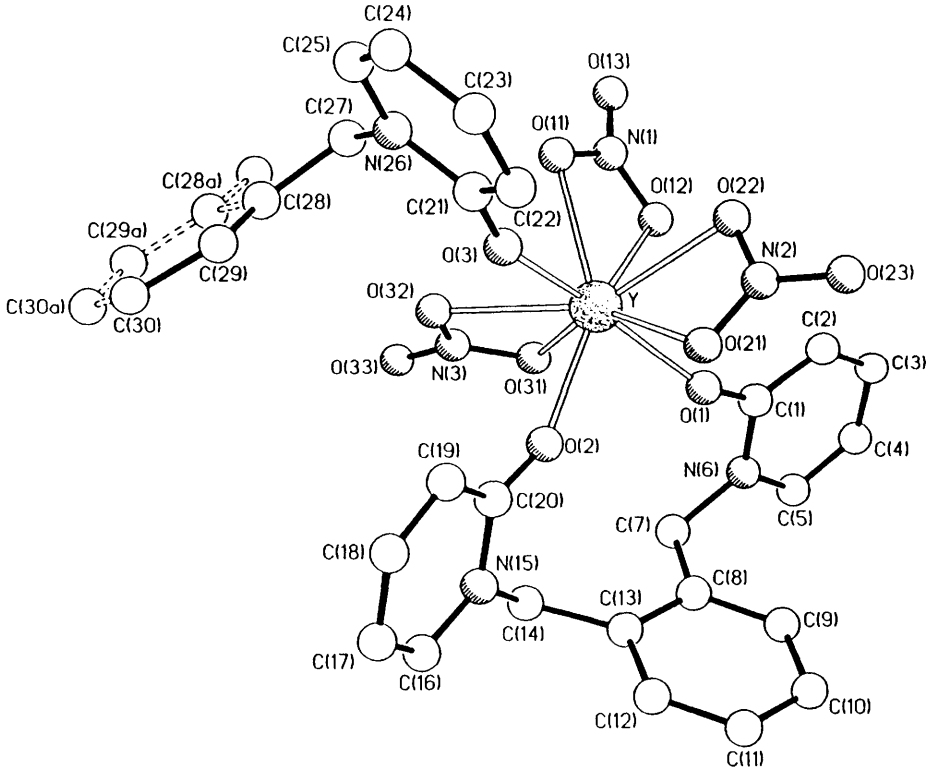

Fig. 4 The yttrium co-ordination environment in complex **2**

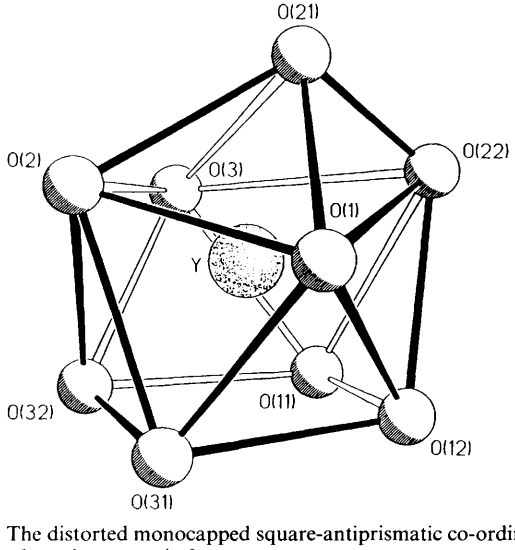

Fig. 5 The distorted monocapped square-antiprismatic co-ordination about each yttrium atom in **2**

its low-frequency IR spectrum, which shows ν(CoCl) bands at 341 cm^{-1} (strong, ν_{asym}) and 307 cm^{-1} (medium, ν_{sym}), as expected[10] for that geometry. The vibrational spectra of the zinc halide complexes are also consistent with tetrahedral co-ordination: chloride, IR 332s and 302m cm^{-1}, Raman 330w and 302s cm^{-1}; bromide, IR 258 cm^{-1} (ν_{sym} hidden by ligand bands 230–220 cm^{-1}, the lower limit of the spectrometer).

In contrast, the IR spectrum of the manganese chloride complex, Mn(*o*-xbp)Cl_2·MeOH, has no ν(MnCl) bands > 200 cm^{-1}, indicating[10] a polymeric structure involving chloride bridges and six-co-ordinate manganese(II). The X-band EPR spectrum of the solid complex (a single band centred on $g = 2$) is consistent with this.[11] Moreover, the complex shows pink luminescence under UV excitation rather than the yellow-green luminescence often observed for tetrahedral Mn^{II} environments. The IR spectrum of the iron(III) chloride complex has a strong band at 375 cm^{-1} indicating[12] the presence of the $FeCl_4^-$ ion, and its formulation as [Fe(*o*-xbp)$_2$$Cl_2$][$FeCl_4$]·MeOH, analogous to *e.g.* [Fe(OPPh$_3$)$_4$$Cl_2$][$FeCl_4$][13] and [Fe{$Ph_2$-P(O)$CH_2CH_2$P(O)$Ph_2$}$_2$$Cl_2$][$FeCl_4$].[14]

The spectroscopic methods provide information about the metal–ion environments in these compounds but not about the longer-range structures adopted by use of ligands such as *o*-xbp. Accordingly, single crystal X-ray diffraction studies have been made on Zn(*o*-xbp)Cl_2 **3**, [Fe(*o*-xbp)$_2$$Cl_2$][$FeCl_4$]·MeOH **4** and [Co(*o*-xbp)$_2$(MeOH)$_2$]I_2·2MeOH **5**.

Structure of Zn(*o*-xbp)Cl_2 **3**.—The X-ray study of **3** shows it to be dimeric, with two *o*-xbp ligands bridging two tetrahedrally co-ordinated zinc centres to form a centrosymmetric 22-membered ring (Fig. 6). The geometry at each zinc atom is noticeably distorted; the Cl–Zn–Cl angle is enlarged to 121.7(1)° and the O–Zn–O angle is contracted to 103.2(1)°. There are also small differences in the pairs of Zn–O and Zn-Cl bond lengths (Table 10).

The conformational relationship of the pyridone rings with respect to the central *o*-xylene unit is essentially the same as in **1** and **2** (Table 5). However, whereas in **1** and **2** they have either C_s or C_2 symmetry, in **3** the symmetry is C_1. This symmetry lowering is manifested by the relative directions of the C=O bonds. In **1** the two C=O groups of each *o*-xbp ligand are directed towards each other; in **2** that is also true for the chelating *o*-xbp ligand, whilst for the bridging ligand they are directed away from each other; in **3** they are approximately co-directional. It is almost certain that the bridging geometry observed in **2** would not be possible in a ring dimer, as this would result in too close an approach of the *o*-xylene units. In **3**, these rings, though noticeably staggered, approach to within 3.37 Å; the macrocycle is self-filling.

Again, there are no significant intermolecular packing interactions.

Table 6 Atomic coordinates (× 10^4) for compound **2**

Atom	*x*	*y*	*z*	Atom	*x*	*y*	*z*
Y	6782(1)	5157(1)	3715(1)	C(24)	4970(4)	3780(5)	5428(7)
O(1)	7619(2)	5635(3)	3693(3)	C(25)	4857(3)	3930(5)	4640(6)
C(1)	7934(3)	6167(5)	3493(5)	N(26)	5259(3)	4136(3)	4224(4)
C(2)	7947(3)	6997(5)	3710(5)	C(27)	5112(3)	4238(4)	3360(5)
C(3)	8311(4)	7529(5)	3468(6)	C(28)	5073(3)	3438(4)	2912(4)
C(4)	8662(3)	7256(6)	2975(6)	C(29)	5142(3)	2692(5)	3307(5)
C(5)	8643(3)	6466(5)	2758(5)	C(30)	5071(4)	1956(5)	2903(5)
N(6)	8290(3)	5933(4)	3011(4)	N(1)	6145(3)	6589(5)	3121(5)
C(7)	8277(3)	5073(4)	2753(5)	O(11)	5945(2)	5938(4)	3353(4)
C(8)	8576(3)	4500(5)	3375(5)	O(12)	6647(3)	6585(3)	3174(4)
C(9)	9025(4)	4795(6)	3887(6)	O(13)	5868(3)	7163(4)	2865(5)
C(10)	9322(4)	4284(7)	4452(7)	N(2)	7186(3)	5688(6)	5281(5)
C(11)	9178(4)	3471(7)	4497(7)	O(21)	7269(2)	4977(4)	5061(4)
C(12)	8736(4)	3194(5)	3997(6)	O(22)	6840(3)	6104(4)	4822(4)
C(13)	8428(3)	3687(5)	3430(5)	O(23)	7438(3)	5971(4)	5909(4)
C(14)	7956(3)	3299(4)	2878(5)	N(3)	6476(3)	4688(4)	2053(5)
N(15)	7617(2)	2805(3)	3313(4)	O(31)	6858(2)	5182(4)	2288(3)
C(16)	7682(3)	1969(5)	3347(5)	O(32)	6223(2)	4437(4)	2565(4)
C(17)	7402(4)	1512(5)	3766(5)	O(33)	6349(2)	4482(4)	1356(4)
C(18)	7031(4)	1875(6)	4186(5)	N(31)	5513(8)	9921(12)	3125(12)
C(19)	6954(3)	2691(6)	4144(5)	C(32)	5257(9)	9310(15)	2904(13)
C(20)	7248(3)	3192(5)	3702(5)	C(33)	4948(9)	8594(11)	2767(12)
O(2)	7215(2)	3957(3)	3640(3)	N(34)	5593(7)	8243(10)	5044(10)
O(3)	6144(2)	4419(3)	4191(3)	N(34′)	5899(10)	9974(15)	3738(15)
C(21)	5792(3)	4210(4)	4594(5)	C(35)	5916(10)	8345(13)	4732(13)
C(22)	5912(3)	4037(4)	5416(5)	C(35′)	6138(16)	9333(27)	4144(25)
C(23)	5502(4)	3829(5)	5815(5)	C(36)	6365(7)	8538(13)	4410(9)

Table 7 Selected bond lengths (Å) and angles (°) with e.s.d.s in parentheses for complex **2**

Y–O(1)	2.240(6)	Y–O(2)	2.250(6)
Y–O(3)	2.259(6)	Y–O(11)	2.433(6)
Y–O(12)	2.506(6)	Y–O(21)	2.423(6)
Y–O(22)	2.427(7)	Y–O(31)	2.482(6)
Y–O(32)	2.494(7)		
O(1)–Y–O(2)	80.9(2)	O(1)–Y–O(3)	155.8(2)
O(2)–Y–O(3)	86.3(2)	O(1)–Y–O(11)	125.2(2)
O(2)–Y–O(11)	147.2(2)	O(3)–Y–O(11)	75.0(2)
O(1)–Y–O(12)	74.6(2)	O(2)–Y–O(12)	145.2(2)
O(3)–Y–O(12)	124.8(2)	O(11)–Y–O(12)	50.7(2)
O(1)–Y–O(21)	75.2(2)	O(2)–Y–O(21)	77.5(2)
O(3)–Y–O(21)	82.0(2)	O(11)–Y–O(21)	124.7(2)
O(12)–Y–O(21)	118.4(2)	O(1)–Y–O(22)	82.3(2)
O(2)–Y–O(22)	129.4(2)	O(3)–Y–O(22)	90.3(2)
O(11)–Y–O(22)	78.2(2)	O(12)–Y–O(22)	71.5(2)
O(21)–Y–O(22)	52.1(2)	O(1)–Y–O(31)	75.1(2)
O(2)–Y–O(31)	80.6(2)	O(3)–Y–O(31)	123.0(2)
O(11)–Y–O(31)	87.3(2)	O(12)–Y–O(31)	69.5(2)
O(21)–Y–O(31)	145.4(2)	O(22)–Y–O(31)	138.8(2)
O(1)–Y–O(32)	123.0(2)	O(2)–Y–O(32)	75.8(2)
O(3)–Y–O(32)	72.7(2)	O(11)–Y–O(32)	73.1(2)
O(12)–Y–O(32)	97.2(2)	O(21)–Y–O(32)	144.0(2)
O(22)–Y–O(32)	149.5(2)	O(31)–Y–O(32)	50.4(2)
Y–O(1)–C(1)	151.2(5)	Y–O(2)–C(20)	152.3(5)
Y–O(3)–C(21)	161.5(5)	Y–O(12)–N(1)	95.7(5)
Y–O(11)–N(1)	98.6(5)	Y–O(21)–N(2)	95.2(5)
Y–O(22)–N(2)	94.8(6)	Y–O(31)–N(3)	96.8(5)
Y–O(32)–N(3)	96.8(5)		

The X-ray powder pattern of the bromide analogue is very similar to that of **3**; there are small differences in line positions but it appears that the gross structures of the two compounds are the same, though they are not strictly isostructural.

Structure of Fe(*o*-xbp)Cl_3·0.5MeOH **4**.—The X-ray diffraction study on **4** shows that the complex does indeed have the composition [Fe(*o*-xbp)$_2$$Cl_2$][$FeCl_4$]·MeOH. The cation comprises an essentially undistorted *cis*-octahedral FeO_4Cl_2 co-ordination geometry, with two chelating *o*-xbp ligands (Fig. 7; Table 12). Despite the difference in the main co-ordination geometry, the gross structure of **4** is remarkably similar to that adopted by **1**. The complex cation in **4** possesses approximate molecular C_2 symmetry about an axis passing through the iron atom and bisecting the Cl–Fe–Cl angle. The *o*-xbp ligand conformations again resemble very closely those in **1** and the chelating ligand in **2** (torsion angles are listed in Table 5).

As in **1**, there is pronounced inter-ligand stabilisation produced by pyridone–xylene ring edge-to-face interactions. These again occur between the pyridone ring C(1)–N(6) and the xylene ring C(28)–C(33) and between the pyridone N(35)–C(40) and the aryl C(8)–C(13). The centroid–centroid ring separations are *ca.* 5 Å and the centroid–centroid vectors subtend angles of *ca.* 80° to the respective xylene ring planes.

An analysis of the packing of the cations and anions in **4** shows the tetrahedral $FeCl_4^-$ ions to be localised in sheets perpendicular to the *b* crystallographic direction (Fig. 8). The only significant intermolecular interaction is a parallel, and overlapping, stacking of pairs of pyridone rings (interplanar separation *ca.* 3.4 Å).

The solvate, occluded methanol molecules are quite readily lost from the crystals after isolation.

Structure of [Co(*o*-xbp)$_2$(MeOH)$_2$]I_2·2MeOH **5**.—Reactions of cobalt(II) bromide or iodide with *o*-xbp in methanol-dmp solution gave purple compounds, which, from microanalytical data appeared to be Co(*o*-xbp)$_2$$X_2$ (X = Br or I) but with several methanol and/or water molecules of solvation. The microanalytical results were rather inconsistent and the compounds tended to desolvate on exposure to the atmosphere. Good crystals were obtained for the iodide, so this was characterised by single crystal X-ray diffraction.

The X-ray results showed that the crystalline sample has the stoichiometry Co(*o*-xbp)$_2$$I_2$·4MeOH with *trans*-octahedral geometry, comprising two chelating *o*-xbp ligands and

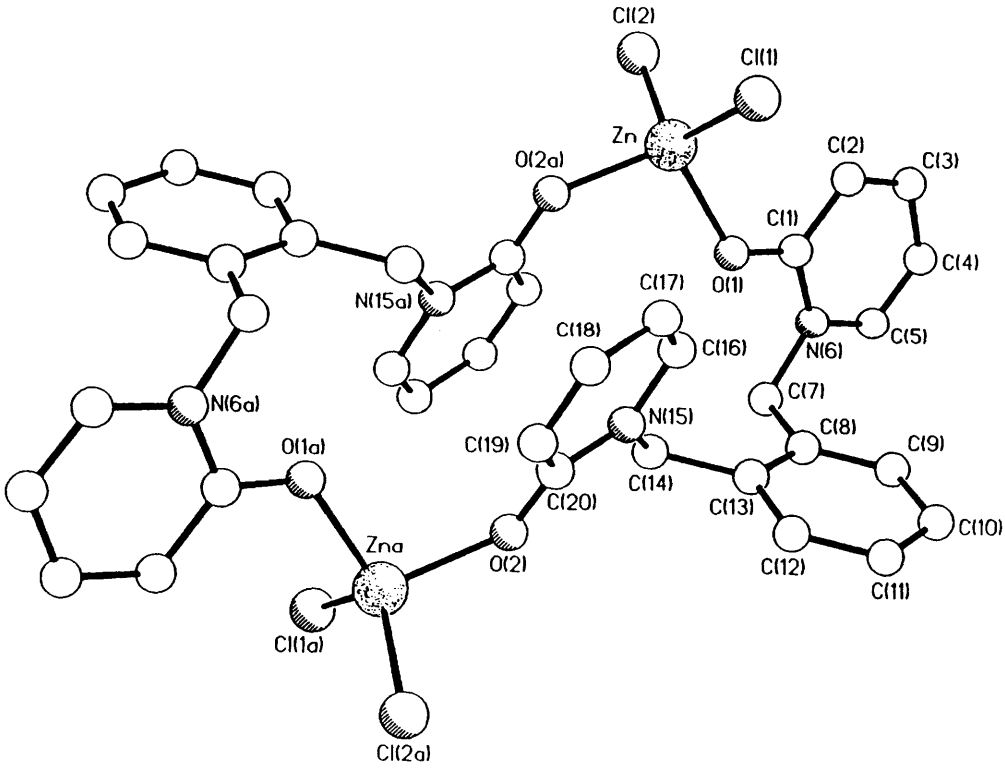

Fig. 6 The dinuclear ring structure of complex **3**

Table 8 Phosphorescence emission spectra of solid samples of $[M_2(o\text{-xbp})_3(NO_3)_6]$ (M = Sm, Eu, Tb or Dy)

M	Excitation (nm)	Phosphorescent emission (nm)	Lifetime (μs)[a]
Sm	377	563.5 ($^4G_{\frac{5}{2}} \longrightarrow {}^6H_{\frac{5}{2}}$), 598 ($^6H_{\frac{7}{2}}$), 642.5 ($^6H_{\frac{9}{2}}$)	*b*
Eu	397	593 ($^5D_0 \longrightarrow {}^7F_1$), 617 ($^7F_2$)	880
Tb	320	491 ($^5D_4 \longrightarrow {}^7F_6$). 545.5 ($^7F_5$), 583.5 ($^7F_4$), 621.5 ($^7F_3$)	1100
Dy	366	481 ($^4F_{\frac{9}{2}} \longrightarrow {}^6H_{\frac{15}{2}}$), 574.5 ($^6H_{\frac{13}{2}}$)	41

[a] Measured from 617 nm band (Eu), 545.5 nm band (Tb) or 574.5 nm band (Dy). [b] Phosphorescent emission too weak for reliable lifetime measurement.

Table 9 Atomic coordinates (× 10^4) for compound **3**

Atom	*x*	*y*	*z*
Zn	3 685(1)	1 168(1)	1 761(1)
Cl(1)	3 392(1)	2 176(1)	2 650(1)
Cl(2)	2 498(1)	899(1)	−305(1)
O(1)	5 895(2)	1 053(1)	2 010(2)
O(2)	3 144(2)	441(1)	2 919(2)
C(1)	6 674(3)	1 298(1)	1 238(3)
C(2)	6 213(4)	1 805(2)	257(3)
C(3)	7 112(4)	2 023(2)	−530(3)
C(4)	8 533(4)	1 732(2)	−388(3)
C(5)	8 976(4)	1 248(2)	547(3)
N(6)	8 082(3)	1 040(1)	1 373(2)
C(7)	8 662(3)	552(2)	2 460(3)
C(8)	9 220(3)	915(1)	3 792(3)
C(9)	10 295(3)	1 421(2)	3 861(3)
C(10)	10 933(3)	1 749(2)	5 045(3)
C(11)	10 511(3)	1 564(2)	6 204(3)
C(12)	9 434(4)	1 066(2)	6 148(3)
C(13)	8 754(3)	746(1)	4 956(3)
C(14)	2 471(3)	−227(2)	5 037(3)
N(15)	3 498(2)	−499(1)	4 245(2)
C(16)	4 188(3)	−1 115(2)	4 637(3)
C(17)	5 097(4)	−1 409(2)	3 941(3)
C(18)	5 316(3)	−1 081(2)	2 791(3)
C(19)	4 652(3)	−472(2)	2 401(3)
C(20)	3 736(3)	−144(1)	3 159(3)

Table 10 Selected bond lengths (Å) and angles (°) with e.s.d.s in parentheses for complex **3**

Zn–Cl(1)	2.208(2)	Zn–Cl(2)	2.220(2)
Zn–O(1)	2.005(2)	Zn–O(2)	1.982(2)
Cl(1)–Zn–Cl(2)	121.7(1)	Cl(1)–Zn–O(1)	105.1(1)
Cl(2)–Zn–O(1)	111.3(1)	Cl(1)–Zn–O(2)	108.4(1)
Cl(2)–Zn–O(2)	105.6(1)	O(1)–Zn–O(2)	103.2(1)
Zn–O(1)–C(1)	125.2(2)	Zn–O(2)–C(20)	127.3(2)

two axially disposed co-ordinated methanol molecules (Fig. 9).

The complex has crystallographic C_2 symmetry about an axis perpendicular to, and bisecting, the C(3)–O(3a) vector. The Co–O bond lengths are in the range 2.089(4)–2.112(4) Å (Table 14), there being no significant difference between the axial and equatorial bond distances. Distortions from O_h symmetry are small, with the angles at Co in the ranges 87.9(1)–94.4(2) and 177.1(2)–178.9(3)°. In common with the arrangements observed in **1**, **2** and **4** the chelating *o*-xbp ligands have non-crystallographic C_s symmetry (relevant torsion angles are given in Table 5).

The axially co-ordinated methanol molecules are each hydrogen bonded to discrete methanol solvate molecules

Table 11 Atomic coordinates (× 10^4) for compound **4**

Atom	*x*	*y*	*z*	Atom	*x*	*y*	*z*
Fe(1)	−3934(4)	−723(5)	−1480(3)	C(22)	−1945(23)	−30(33)	−2012(15)
Cl(1)	−3957(7)	1509(8)	−1547(4)	C(23)	−1368(27)	787(42)	−2126(18)
Cl(2)	−4082(6)	−1076(8)	−2383(4)	C(24)	−991(26)	1611(40)	−1735(18)
O(1)	−3935(15)	−2650(20)	−1338(9)	C(25)	−1114(25)	1657(38)	−1291(17)
C(1)	−3459(21)	−3483(32)	−1054(14)	N(26)	−1744(17)	887(27)	−1129(11)
C(2)	−2671(23)	−3367(37)	−684(15)	C(27)	−1977(21)	1014(31)	−630(13)
C(3)	−2298(26)	−4313(41)	−375(17)	C(28)	−1624(22)	−102(31)	−251(14)
C(4)	−2681(22)	−5503(36)	−457(14)	C(29)	−950(24)	−807(36)	−302(15)
C(5)	−3398(23)	−5668(37)	−822(14)	C(30)	−630(22)	−1810(32)	39(14)
N(6)	−3819(17)	−4694(26)	−1122(11)	C(31)	−1066(23)	−2061(34)	433(15)
C(7)	−4640(21)	−4892(31)	−1508(13)	C(32)	−1736(25)	−1259(37)	496(16)
C(8)	−5359(20)	−4385(32)	−1320(13)	C(33)	−2015(20)	−327(33)	134(13)
C(9)	−5568(23)	−4874(33)	−876(15)	C(34)	−2820(23)	330(37)	222(16)
C(10)	−6265(24)	−4564(37)	−658(16)	N(35)	−3563(16)	−454(26)	212(11)
C(11)	−6827(26)	−3645(38)	−938(16)	C(36)	−3811(24)	−763(35)	645(16)
C(12)	−6667(25)	−3181(35)	−1401(16)	C(37)	−4501(24)	−1504(34)	640(16)
C(13)	−5980(22)	−3492(31)	−1580(13)	C(38)	−4931(25)	−1922(33)	140(15)
C(14)	−5827(21)	−3000(29)	−2099(13)	C(39)	−4685(22)	−1668(32)	−317(14)
N(15)	−6226(18)	−1658(24)	−2242(11)	C(40)	−3987(19)	−765(29)	−308(13)
C(16)	−6912(24)	−1532(35)	−2646(15)	O(4)	−3727(13)	−521(21)	−703(9)
C(17)	−7244(21)	−344(35)	−2822(13)	C(41)	−1217(62)	−52(93)	1999(38)
C(18)	−6823(25)	715(39)	−2597(15)	O(42)	−2049(27)	275(38)	1654(16)
C(19)	−6161(22)	578(35)	−2144(14)	Fe(2)	167(6)	−1052(8)	3803(4)
C(20)	−5750(23)	−636(37)	−1952(15)	Cl(3)	1041(8)	−2259(13)	4351(6)
O(2)	−5191(13)	−838(20)	−1528(9)	Cl(4)	792(12)	258(15)	3414(7)
O(3)	−2662(15)	−726(22)	−1346(9)	Cl(5)	−462(14)	188(18)	4334(12)
C(21)	−2148(22)	−47(32)	−1522(15)	Cl(6)	−853(17)	−2051(19)	3337(13)

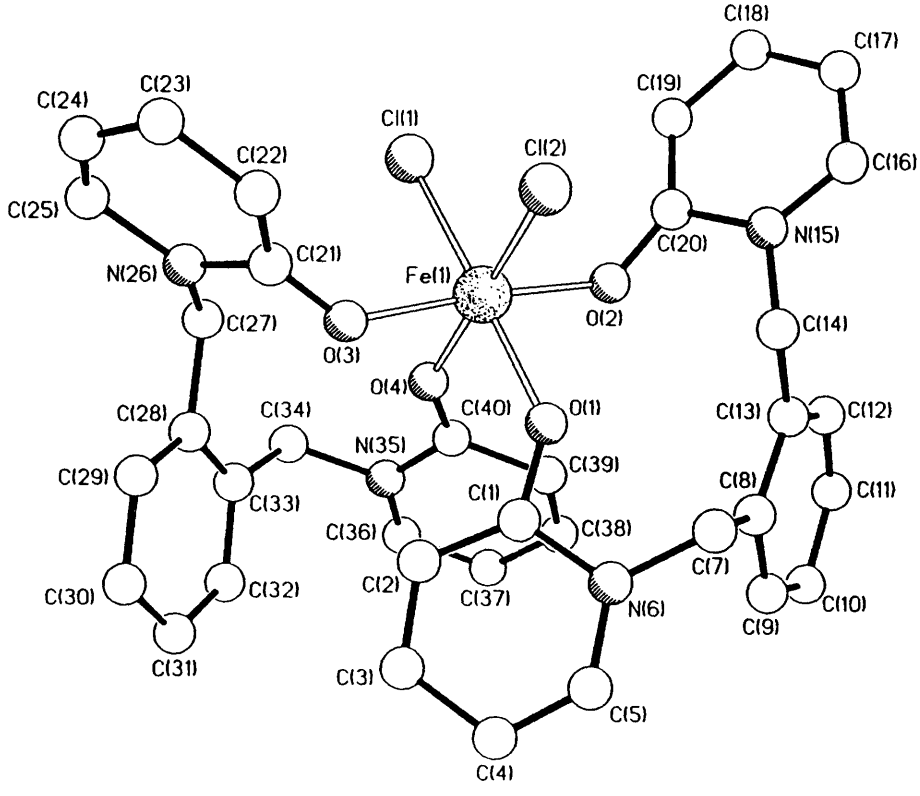

Fig. 7 The structure of the cation in complex **4** showing the *cis*-octahedral co-ordination geometry about the iron atom

[O(3)···O(4) 2.68 Å]; these are, in turn, hydrogen bonded to the iodide ions [O(4)···I 3.41 Å]. The only other intermolecular interactions of note are ligand–ligand aromatic edge-to-face interactions. These are between the edge of heterocycle N(15)–C(20) in one molecule and the face of the *ortho*-phenyl ring in another (centroid–centroid separation 4.9 Å, centroid–centroid vector inclined by 87° to the aromatic ring plane).

A pattern that emerges from these studies is that, despite the apparent structural diversity in the structures of the five representative complexes with *o*-xbp, the conformational preferences of that ligand induce a greater constancy of ligand

Table 12 Selected bond lengths (Å) and angles (°) with e.s.d.s in parentheses for complex **4**

Fe(1)–Cl(1)	2.367(10)	Fe(1)–Cl(2)	2.324(12)
Fe(1)–O(1)	2.071(22)	Fe(1)–O(2)	2.005(23)
Fe(1)–O(3)	1.997(24)	Fe(1)–O(4)	1.969(24)
Fe(2)–Cl(4)	2.109(22)	Fe(2)–Cl(3)	2.158(16)
Fe(2)–Cl(6)	2.077(26)	Fe(2)–Cl(5)	2.307(29)
Cl(1)–Fe(1)–Cl(2)	95.2(4)	Cl(1)–Fe(1)–O(1)	173.7(8)
Cl(2)–Fe(1)–O(1)	90.9(7)	Cl(1)–Fe(1)–O(2)	93.4(7)
Cl(2)–Fe(1)–O(2)	94.2(7)	O(1)–Fe(1)–O(2)	84.7(9)
Cl(1)–Fe(1)–O(3)	90.6(8)	Cl(2)–Fe(1)–O(3)	91.3(8)
O(1)–Fe(1)–O(3)	90.7(10)	O(2)–Fe(1)–O(3)	172.8(10)
Cl(1)–Fe(1)–O(4)	87.9(7)	Cl(2)–Fe(1)–O(4)	175.2(7)
O(1)–Fe(1)–O(4)	86.2(10)	O(2)–Fe(1)–O(4)	89.3(9)
O(3)–Fe(1)–O(4)	84.9(9)	Fe(1)–O(1)–C(1)	139.0(21)
Fe(1)–O(2)–C(20)	123.0(25)	Fe(1)–O(3)–C(21)	132.4(21)
Fe(1)–O(4)–C(40)	145.5(20)	Cl(3)–Fe(2)–Cl(4)	113.0(7)
Cl(3)–Fe(2)–Cl(5)	104.9(9)	Cl(4)–Fe(2)–Cl(5)	104.0(8)
Cl(3)–Fe(2)–Cl(6)	112.3(8)	Cl(4)–Fe(2)–Cl(6)	117.4(11)
Cl(5)–Fe(2)–Cl(6)	103.6(11)		

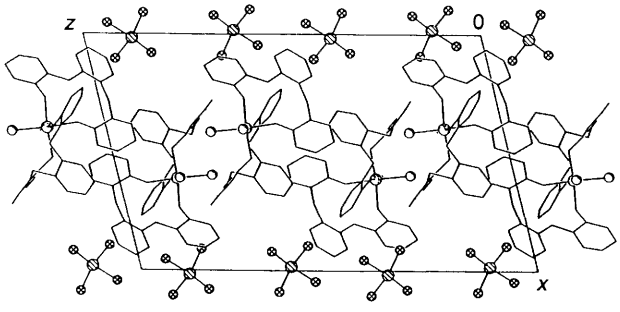

Fig. 8 View down the crystallographic *b* direction in the structure of **4** showing the localisation of the $FeCl_4^-$ ions in sheets in the lattice

geometry than might at first seem to be the case. Although the ligand will function as a bridge between metal ions, it appears that the *ortho*-xylene link-unit between the pyridone rings tends to favour chelation, despite the large size (eleven-membered) of the resulting chelate ring.

Table 13 Atomic coordinates (× 10^4) for compound **5**

Atom	*x*	*y*	*z*
Co	5000	−4136(1)	2500
O(1)	5517(2)	−5693(4)	3180(2)
C(1)	5317(3)	−6741(6)	3409(2)
C(2)	4689(3)	−7465(7)	3134(3)
C(3)	4525(4)	−8626(7)	3412(3)
C(4)	4984(4)	−9133(7)	3979(3)
C(5)	5577(4)	−8413(7)	4252(3)
N(6)	5746(3)	−7235(5)	3987(2)
C(7)	6390(3)	−6447(6)	4330(3)
C(8)	6248(3)	−5085(6)	4618(3)
C(9)	5979(3)	−5212(8)	5064(3)
C(10)	5831(4)	−4017(8)	5340(3)
C(11)	5967(4)	−2658(8)	5182(3)
C(12)	6240(3)	−2513(7)	4750(3)
C(13)	6384(3)	−3695(6)	4456(3)
C(14)	6695(3)	−3528(6)	3986(3)
N(15)	6632(3)	−2047(5)	3741(2)
C(16)	7175(3)	−1110(8)	3970(3)
C(17)	7120(4)	252(7)	3756(3)
C(18)	6525(4)	662(7)	3292(3)
C(19)	5983(4)	−250(7)	3060(3)
C(20)	6010(3)	−1665(7)	3293(3)
O(2)	5517(2)	−2531(4)	3137(2)
O(3)	4191(2)	−4114(6)	2795(2)
C(21)	4160(5)	−3341(11)	3288(4)
O(4)	3126(3)	−5949(8)	2376(3)
C(22)	2834(5)	−6514(16)	2751(5)
I	1803(1)	−5979(1)	969(1)

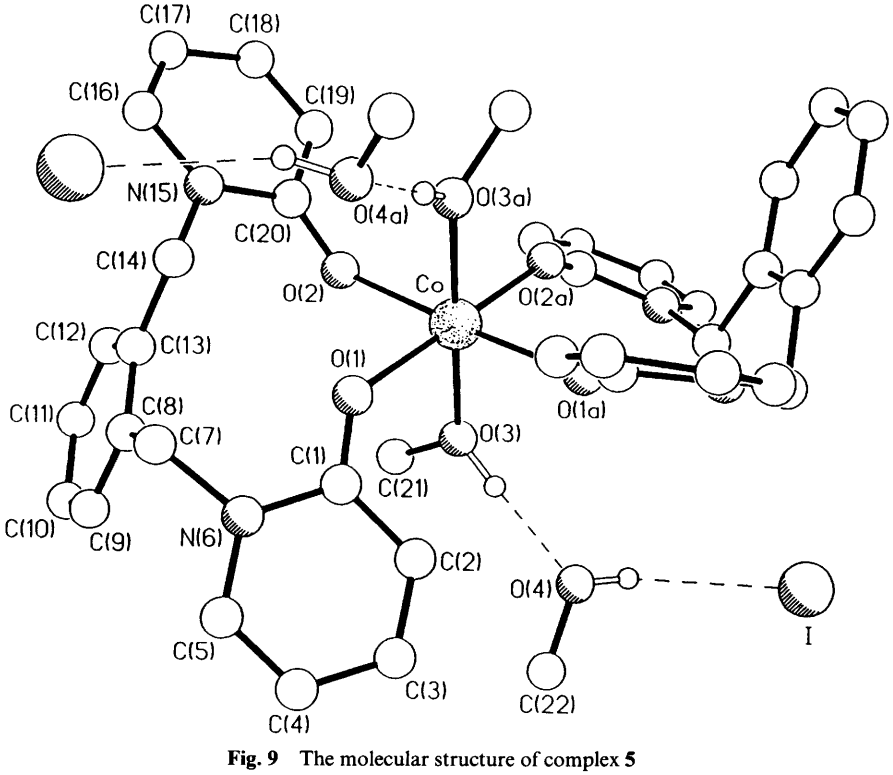

Fig. 9 The molecular structure of complex **5**

Table 14 Selected bond lengths (Å) and angles (°) with e.s.d.s in parentheses for complex **5**

Co–O(1)	2.112(4)	Co–O(2)	2.089(4)
Co–O(3)	2.093(6)	Co–O(1′)	2.112(4)
Co–O(2′)	2.089(4)	Co–O(3′)	2.093(6)
O(1)–Co–O(2)	87.9(1)	O(1)–Co–O(3)	90.3(2)
O(2)–Co–O(3)	91.3(2)	O(1)–Co–O(1′)	94.4(2)
O(2)–Co–O(1′)	177.1(2)	O(3)–Co–O(1′)	90.5(2)
O(1)–Co–O(2′)	177.1(2)	O(2)–Co–O(2′)	89.8(2)
O(3)–Co–O(2′)	87.9(2)	O(1′)–Co–O(2′)	87.9(1)
O(1)–Co–O(3′)	90.5(2)	O(2)–Co–O(3′)	87.9(2)
O(3)–Co–O(3′)	178.9(3)	O(1′)–Co–O(3′)	90.3(2)
O(2′)–Co–O(3′)	91.3(2)	Co–O(1)–C(1)	133.2(4)
Co–O(2)–C(20)	143.8(5)	Co–O(3)–C(21)	126.8(5)

Acknowledgements

We thank the SERC for Research Studentships (to S. P. W. H. and A. M. S.) and for the diffractometers and EPR spectrometer.

References

1 G. A. Doyle, D. M. L. Goodgame, S. P. W. Hill and D. J. Williams, *J. Chem. Soc., Chem Commun.*, 1993, 207.
2 D. M. L. Goodgame, S. P. W. Hill and D. J. Williams, *J. Chem. Soc., Chem. Commun.*, 1993, 1019.
3 D. M. L. Goodgame, S. P. W. Hill and D. J. Williams, *Polyhedron*, 1992, **12**, 2933.
4 C. Alberti, *Gazz. Chim. Ital.*, 1956, **86**, 1181.
5 L. H. Carrad, D. M. L. Goodgame, S. P. W. Hill and D. J. Williams, *J. Chem. Soc., Dalton Trans.*, 1993, 1003.
6 G. M. Sheldrick, SHELXTL PC, Version 4.2, Siemens Analytical Instruments Inc., Madison, WI, 1990.
7 D. M. L. Goodgame, D. J. Williams and R. E. P. Winpenny, *Polyhedron*, 1988, **7**, 1807.
8 D. M. L. Goodgame, S. Newnham, C. A. O'Mahoney and D. J. Williams, *Polyhedron*, 1990, **9**, 491.
9 D. M. L. Goodgame and M. Goodgame, *Inorg. Chem.*, 1965, **4**, 139.
10 K. Nakamoto, *Infrared and Raman Spectra of Inorganic and Coordination Compounds*, Wiley, New York, 3rd edn., 1977, Part III, pp. 317–324 and refs. therein.
11 R. D. Dowsing, J. F. Gibson, D. M. L. Goodgame, M. Goodgame and P. J. Hayward, *Nature (London)*, 1968, **219**, 1037.
12 J. S. Avery, C. D. Burbridge and D. M. L. Goodgame, *Spectrochim. Acta, Part A*, 1968, **24**, 1721.
13 E. Durcanská and T. Glowiak, *Acta Crystallogr., Sect. C*, 1989, **45**, 410.
14 D. C. Povey, T. S. Lobana and P. K. Bhatia, *J. Crystallogr. Spectrosc. Res.*, 1991, **21**, 13.

Received 5th November 1993; *Paper* 3/06634G